

Shock-induced phase transition of β -Si₃N₄ to c -Si₃N₄

Hongliang He, T. Sekine,* T. Kobayashi, and H. Hirosaki

National Institute for Research in Inorganic Materials (NIRIM), 1-1 Namiki, Tsukuba, Ibaraki 305-0044, Japan

Isao Suzuki

Department of Earth Science, Okayama University, Okayama 700-8530, Japan

(Received 14 June 2000)

Hugoniot curve (shock velocity vs particle velocity and pressure vs density) of β -Si₃N₄ has been measured up to 150 GPa by a two-stage light gas gun and an inclined-mirror method. The Hugoniot elastic limit is detected to be about 16 GPa. Above ~ 36 GPa, a phase transition from β -Si₃N₄ to c -Si₃N₄ is discovered. The kinetics is very sluggish. This phase transition does not seem to complete at the highest pressure achieved in this work, but an extrapolation gives a pressure of ~ 180 GPa for the completion. Isentrope of c -Si₃N₄ has been determined from the Hugoniot data by fitting the Birch-Murnaghan equation of state. The zero-pressure bulk modulus and its first pressure derivative are found to be 300 ± 10 GPa and 3.0 ± 0.1 , respectively. These values are in agreement with the first-principles calculations, and therefore strongly support that c -Si₃N₄ is a low compressibility phase.

I. INTRODUCTION

Because of its advanced mechanical, electronic, and thermal properties, silicon nitride (Si₃N₄) has been extensively studied.^{1,2} Two basic crystal structures, named α and β , have been known for a long time. Both of them are hexagonal forms, but β phase is slightly denser due to its shorter lattice length in the c -axis direction. Of great interest, a third form of Si₃N₄ with denser, cubic spinel structure (c -Si₃N₄) has been synthesized recently³ at pressures above 15 GPa and temperatures exceeding 2000 K by the diamond anvil cell technique. The first-principles calculations^{3,4} predict that this phase may have many interesting physical properties due to its special coordination of silicon atoms in the octahedra. In particular, it is believed that c -Si₃N₄ is a superhard material due to its low compressibility. The predicted³⁻⁵ zero-pressure bulk modulus and its first pressure derivative at room temperature are 280–300 GPa and 3.48, respectively. They are comparable to those of the hardest known oxide (stishovite).⁶ An experimental measurement on the compression behavior of c -Si₃N₄ is necessary to check these predictions.

Previously, the compression of β -Si₃N₄ has been studied under both static⁷ pressures up to 34 GPa at room temperature and shock⁸ pressures up to 40 GPa, but no phase transformation was reported. Recently, we have demonstrated⁹ that β -Si₃N₄ is transformed into c -Si₃N₄ under shock wave compression using β -Si₃N₄ powders mixed with copper powders as pressure media. The yield of c -Si₃N₄ increases with increasing shock pressure and temperature, and nearly 80% of c -Si₃N₄ can be recovered from the samples subjected to shock at 50 GPa and 2400 K. This observation prompted us to conduct the shock compression measurement on β -Si₃N₄ at pressures higher than 40 GPa, which may throw light on the compressibility of c -Si₃N₄.

In this paper, we report the Hugoniot curve (pressure vs density) of β -Si₃N₄ up to 150 GPa. It is found that the phase transition of β - to c -Si₃N₄ starts at about 36 GPa. Isentrope

of c -Si₃N₄ has been deduced from the Hugoniot data. The results give a bulk modulus and its first pressure derivative of 300 ± 10 GPa and 3.0 ± 0.1 , respectively, at zero pressure and room temperature, indicating that c -Si₃N₄ is a low compressibility phase.

II. EXPERIMENTAL METHOD

Two kinds of β -Si₃N₄ sintered blocks were used as the target material. They were fabricated by one of the authors (H. Hirosaki). The first one is black (hereafter called SN-A for simplification); the average grain size is about 2 μ m. Sintering additives are Nd₂O₃ and Y₂O₃ with total amount of 2 wt.%. The second gray block (SN-B) is a nearly pure β -Si₃N₄ with the grain size of 0.5 μ m and no additive. The plate-shaped samples with size of about 10 mm \times 12 mm \times (2.5–3) mm were cut out from these blocks, and then lapped and polished on both sides. The mean bulk density was 3.236 g/cm³ for SN-A and 3.184 g/cm³ for SN-B with an accuracy of 0.2% by the Archimedian method. The measured density of SN-B is very close to the x-ray density of β -Si₃N₄ (3.200 g/cm³).¹⁰ A sphere with a diameter of about 3.7 mm was used for measurement of elastic properties.¹¹ Ultrasonic data of SN-B at ambient state are listed in Table I.

An inclined mirror method¹² was employed to measure the shock velocity and free-surface velocity of the shock

TABLE I. Ultrasonic data of β -Si₃N₄ (SN-B sample) at ambient state.

| | | |
|-----------------------------|-------|-------------------|
| Density | 3.184 | g/cm ³ |
| Longitudinal sound velocity | 11.17 | km/s |
| Transverse sound velocity | 6.22 | km/s |
| Bulk sound velocity | 8.55 | km/s |
| Bulk modulus | 232.7 | GPa |
| Shear modulus | 123.2 | GPa |
| Poisson's ratio | 0.275 | |

TABLE II. Shock compression results of β -Si₃N₄ by the inclined-mirror method.

| Shot no. | Initial density (g/cm ³) | Impact plate ^a | Driver plate ^a | Impact velocity (km/s) | First wave | | | | Second wave | | | | Third wave | | | |
|--------------------|--------------------------------------|---------------------------|---------------------------|------------------------|-----------------------|--------------------------|----------------|------------------------------|-----------------------|--------------------------|----------------|------------------------------|-----------------------|--------------------------|----------------|------------------------------|
| | | | | | Shock velocity (km/s) | Particle velocity (km/s) | Pressure (GPa) | Density (g/cm ³) | Shock velocity (km/s) | Particle velocity (km/s) | Pressure (GPa) | Density (g/cm ³) | Shock velocity (km/s) | Particle velocity (km/s) | Pressure (GPa) | Density (g/cm ³) |
| T-141 | 3.240 | A | B | 3.67 | 11.21 | 0.422 | 15.3 | 3.367 | 9.39 | 0.668 | 22.8 | 3.462 | | | | |
| T-137 | 3.244 | A | A | 3.08 | 11.30 | 0.437 | 16.0 | 3.374 | 9.90 | 1.053 | 35.7 | 3.609 | 9.01 | 1.888 | 59.7 | 4.034 |
| T-134 | 3.218 | A | A | 3.87 | 11.33 | 0.443 | 16.1 | 3.349 | 9.79 | 1.089 | 36.3 | 3.597 | 8.34 | 2.483 | 72.7 | 4.454 |
| T-143 | 3.197 | A | A | 3.95 | 11.30 | 0.456 | 16.5 | 3.331 | 9.64 | 1.087 | 35.8 | 3.577 | 8.40 | 2.545 | 73.9 | 4.467 |
| T-148 ^b | 3.184 | A | A | 4.64 | 11.49 | 0.455 | 16.6 | 3.315 | 9.75 | 1.104 | 36.7 | 3.564 | 8.92 | 3.012 | 89.8 | 4.715 |
| T-145 | 3.262 | A | A | 4.69 | 11.21 | 0.436 | 15.9 | 3.394 | 9.91 | 1.079 | 36.6 | 3.641 | 9.07 | 3.020 | 93.1 | 4.809 |
| T-140 | 3.244 | A | A | 5.30 | 11.38 | 0.459 | 17.0 | 3.380 | 10.03 | 1.089 | 37.3 | 3.618 | 9.75 | 3.410 | 110.1 | 4.942 |
| T-144 | 3.244 | C | C | 5.14 | 11.47 | 0.455 | 17.0 | 3.378 | 10.29 | 3.907 | 131.7 | 5.204 | | | | |
| T-149 | 3.238 | C | C | 5.52 | 11.56 | 0.451 | 16.9 | 3.369 | 10.88 | 4.172 | 147.7 | 5.237 | | | | |

^aMaterial of impact and driver plates: (A) sus 304 stainless steel; (B) polycarbonate, (C) tungsten.

^bSN-B sample was used in this shot, and SN-A samples in the other shots.

compressed sample using an image converter streak camera (Ultra nac FS 501). The sweep rate of the streak camera was 55 ns/mm, which was calibrated against a modulated laser diode beam trace. A flyer plate (22 mm in diameter) was accelerated to high velocity by a two-stage light-gas gun,¹³ and then impacted onto the sample assembly. Polycarbonate, stainless steel (sus304) and tungsten were used for the flyer and driver plates, for which the shock velocity and particle velocity relationships are well known.¹⁴ The impact velocity was measured by the cutting cw x-ray beam method with an accuracy of 0.3%.

Shock pressure and sample density were calculated from the Rankine-Hugoniot equations¹⁵ based on the measured shock velocity and particle velocity (approximated as the half of the free-surface velocity). In the case of a multi-wave shock, the final shock compression state has been checked with the impedance-match solution.¹⁶

III. EXPERIMENTAL RESULTS

Impact velocity was varied between 3.0 and 5.5 km/s, corresponding to the shock pressures 28–150 GPa in the sample. Results of the experimental measurements are summarized in Table II. Multishock structures were observed on the streak camera records. A two-wave structure was seen below ~ 36 GPa. Beyond this pressure, however, a three-wave structure was observed to a shock pressure of about 110 GPa. Figure 1 is a typical streak camera photograph for SN-B sample (shot T-148) at a final shock pressure 89.8 GPa. Three waves are clearly indicated, and they represent an elastic wave, a plastic wave and a mixed phase wave. The transition points of elastic-plastic and plastic-mixed phase waves are determined by the intersections of the straight lines drawn along the trace of each wave, respectively, from an amplified photograph (see the diagram at the right side in Fig. 1). The determined results from different shots are consistent as indicated in Fig. 3 and Table II. The elastic wave velocity is calculated from the time difference between t_1 and t_0 with the known sample thickness. At time t_2 , a clear kink is caused by the elastic-plastic wave transition, and during the time interval ($t_3 - t_2$) a plastic wave is visible. The kink at time t_3 indicates a phase transition (from β -Si₃N₄ to c -Si₃N₄, as shown later), and a mixed phase state maintains

from time t_3 to t_4 . To look at the difference between SN-A and SN-B samples, a shot (T-145) was conducted at nearly the same shock condition as that for shot T-148. However, no apparent difference has been detected as indicated in Table II.

The highest shock pressure achieved in this study was ~ 150 GPa, where both flyer and driver plate were made of tungsten and the impact velocity reached 5.52 km/s. Figure 2 illustrates a streak camera record from this shot (T-149), which indicates a two-wave structure. Calculations show that the first wave is an elastic wave and the second wave corresponds to a mixed phase wave. A slight curvature is seen on the trace of the mixed phase wave, which may be caused by the sluggishness of the phase transformation.

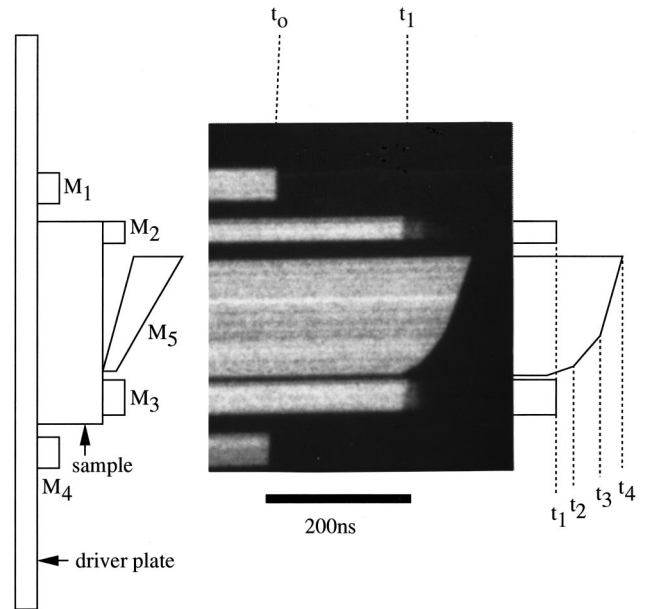


FIG. 1. Sample assembly and the corresponding streak camera record for shot T-148, indicating a three-wave structure. M1 to M4 are flat mirrors and M5 is an inclined mirror with an angle of about 3°. The diagram at the right side is a schematic drawing from the enlarged photograph of streak record. The first, second, and third waves are seen during time intervals $t_0 - t_2$, $t_2 - t_3$, and $t_3 - t_4$, respectively.

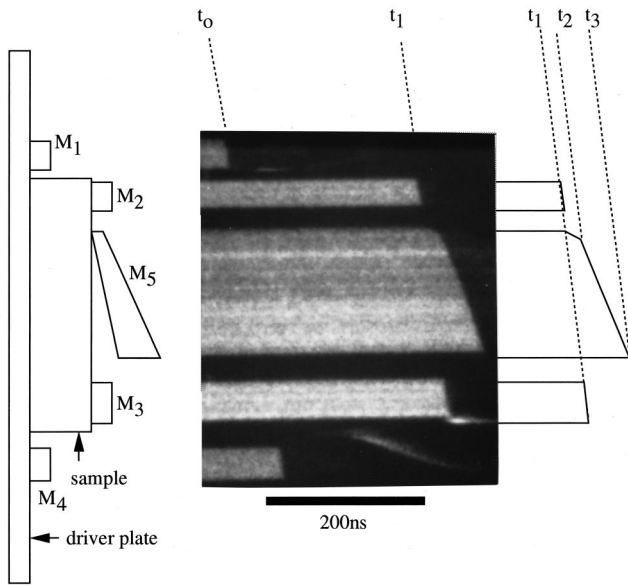


FIG. 2. Sample assembly and the corresponding streak camera record for shot T-149, indicating a two-wave structure. The first and second waves are seen during time intervals t_0-t_1 , and t_1-t_2 , respectively. The trace of mirror M1 is off at a bit early time than M4, which might be due to the shield of the high speed gases leaked from the gun muzzle.

The relation of shock velocity (U_s) versus particle velocity (U_p) is shown in Fig. 3, together with those by Yamakawa *et al.*⁸ For the elastic wave, both U_s and U_p exhibit a good consistence and do not change significantly with the shock pressure. The average elastic wave velocity is 11.36 km/s, which is slightly higher than the longitudinal sound velocity of 11.17 km/s at ambient pressure. Extrapolation

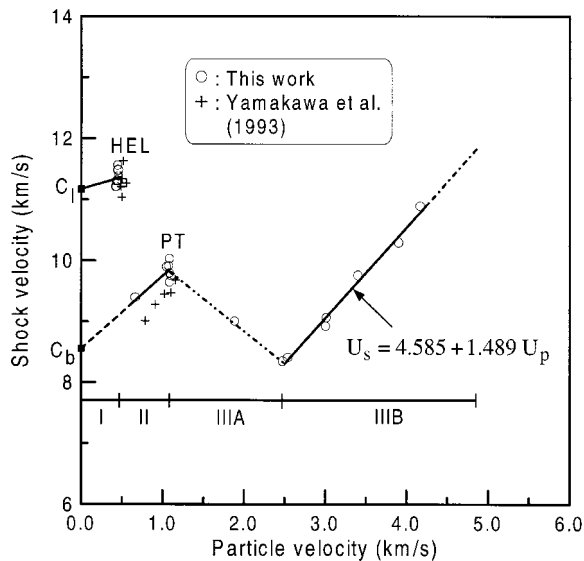


FIG. 3. Shock velocity (U_s) versus particle velocity (U_p). Three regimes are as follows: I, elastic; II, plastic; III(A,B), mixed phase. A best fit to the III(B) regime gives $U_s = 4.585 + 1.489U_p$ with $U_p > 2.5$ km/s. The dashed dot line is an extrapolation of the linear fit. HEL: Hugoniot-elastic limit; PT: phase transition point. C_1 and C_b are the longitudinal and bulk sound velocities (Table I), respectively.

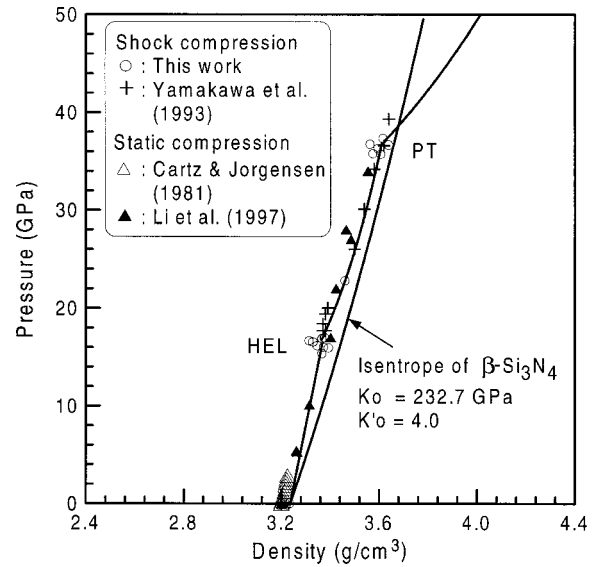


FIG. 4. A comparison of pressure versus density between the shock compression and static measurements under pressures up to 50 GPa. The isentrope of β - Si_3N_4 is computed with Eq. (3).

(the dashed line) of the shock velocity in the plastic regime to $U_p = 0$ km/s shows a result close to the bulk sound wave velocity at ambient state. In the mixed phase regime (IIIB), shock velocity increases with increasing particle velocity, and a best fit gives $U_s = 4.585 + 1.489U_p$ for $U_p > 2.5$ km/s. In regime IIIA, $2.5 > U_p > 1.1$ km/s, the shock velocity is relatively high (shot T-137), which might be associated with a nonequilibrium phase transition behavior in this pressure range. A similar phenomenon was reported for some ceramics.^{17,18} When the shock pressure is high enough, this effect becomes negligible.

Figures 4 and 5 illustrate the pressure and density rela-

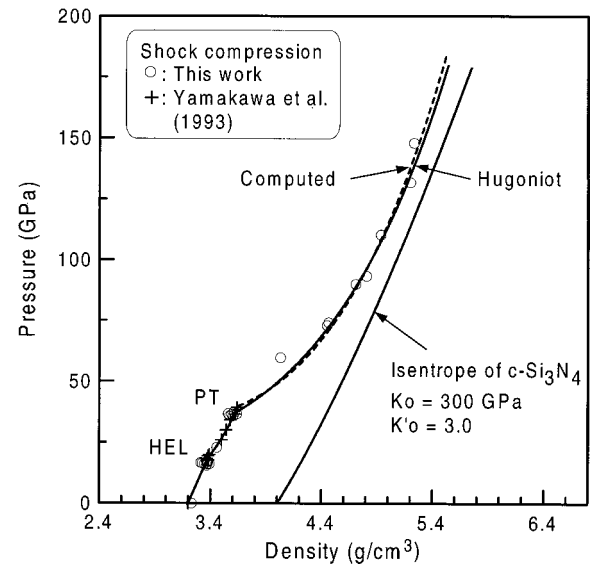


FIG. 5. Pressure-density relation for the shock compression of β - Si_3N_4 up to 150 GPa. The dashed line at pressures above PT is a computed Hugoniot curve which gives the best fit to the experimental Hugoniot data. The indicated isentrope of c - Si_3N_4 is deduced from this computed curve. The solid Hugoniot curve is calculated with the linear $U_s \sim U_p$ relation given in Fig. 3.

tions of shock compressed β -Si₃N₄. The average Hugoniot elastic limit (HEL) and phase transition (PT) pressure are determined to be about 16 and 36 GPa, respectively.

Up to ~ 150 GPa, the observed free-surface trajectories did not show any unstable or double inclined-mirror images, which indicate that the shocked samples (Si₃N₄) are stable and not dissociated.^{18,19} The calculated sample densities from the free-surface velocity measurements also confirm that no low density substances (e.g., nitrogen), are generated under the current shock conditions.

IV. DISCUSSION

A. Phase transition

The phase transition detected by the Hugoniot measurements in the present experiments corresponds to a transformation from β -Si₃N₄ to c -Si₃N₄. We have carried out shock recovery experiments to determine what phase is shock-induced above the transition pressure of 36 GPa.⁹ Recovered samples from β -Si₃N₄ has been converted to a cubic, spinel-type phase.⁹ In those experiments, a powder mixture of β -Si₃N₄ and copper was used as the samples with a bulk porosity of 30–40%. At 21 GPa (temperature 1300 K), β -Si₃N₄ was stable, while at 33 GPa (1800 K), about 30 wt.% of c -Si₃N₄ was recovered from the post-shock samples. Slightly higher transition pressure is observed in this study, which may be attributed to the lower shock temperature generated in the sintered block samples. The calculated shock temperature for the sintered block sample is about 460 K at 36 GPa, which are much lower than that in the recovery experiment.

Up to ~ 150 GPa, a mixed phase regime was observed continuously. This fact indicates that the phase transformation from β - to c -Si₃N₄ is very sluggish. To complete this transformation, higher shock pressures are required. Referring to Fig. 3, one may expect that the end of mixed phase regime will appear if the shock velocity in the mixed phase regime is equal to the elastic wave velocity at HEL. Above that, a single wave structure will appear and it would correspond to one phase regime of c -Si₃N₄. By extrapolating the current measurements to higher pressures (see the dashed dot line in Fig. 3), and assuming 11.8 km/s to be the shock velocity at the end of the mixed phase regime, it is expected that a pressure of about 180 GPa is required to finish this phase transformation in a time interval of 200 to 300 ns, as shown in Figs. 1 and 2.

B. Isentrope of c -Si₃N₄

Given that the shock states between 36 and 180 GPa are attributed to a mixed phase of β -Si₃N₄ and c -Si₃N₄, isentrope of c -Si₃N₄ is reduced from the experimentally determined Hugoniot curve (pressure vs density) in terms of a mixed phase model calculation.^{20–22}

Defining λ as the mass fraction of c -Si₃N₄ in the mixed phase, the specific volume V_m (inverse of density) for the mixed phase is written as

$$V_m = (1 - \lambda)V_1 + \lambda V_2, \quad (1)$$

and by ignoring the interaction effects between the two phases the specific internal energy E_m for the mixed phase is expressed by

$$E_m = (1 - \lambda)E_1 + \lambda E_2, \quad (2)$$

where V_1 , V_2 , E_1 , and E_2 are the corresponding quantities of each phase, subscripts (also in the following equations) 1 and 2 denote β -Si₃N₄ and c -Si₃N₄, respectively.

The third-order Birch-Murnaghan equation of state (EOS) is used to compute the isentropic pressure $P_s(V)$ for each phase,

$$P_s(V) = \frac{3K_0}{2} \left[\left(\frac{V_0}{V} \right)^{7/3} - \left(\frac{V_0}{V} \right)^{5/3} \right] \times \left\{ 1 + \frac{3}{4} (K'_0 - 4) \left[\left(\frac{V_0}{V} \right)^{2/3} - 1 \right] \right\}, \quad (3)$$

where K_0 and K'_0 are the zero-pressure bulk modulus and its first pressure derivative, and V_0 and V are the zero-pressure and high-pressure specific volumes, respectively.

Integration of Eq. (3) gives the isentropic energy $E_s(V)$ as

$$E_s(V) = - \int_{V_0}^V P_s(V) dV, \quad (4)$$

With the assumption that the Hugoniot pressure and shock temperature are common to both phases, a theoretical Hugoniot curve for the mixed phase is constructed on the basis of Eqs. (1)–(4). Grüneisen EOS is applied to relate the isentropic pressure to the Hugoniot pressure for each phase, and gives E_1 (or E_2) being an implicit function of V_1 (or V_2),

$$E_1 = E_s(V_1) + [P_h - P_s(V_1)]V_1/\gamma_1, \quad (5)$$

$$E_2 = E_s(V_2) + [P_h - P_s(V_2)]V_2/\gamma_2 + E_{tr}, \quad (6)$$

where P_h is the Hugoniot pressure, E_{tr} is the transformation energy of β phase to cubic phase at ambient pressure and temperature, and γ is the Grüneisen parameter which is calculated according to the following equation:

$$\frac{\gamma}{V} = \frac{\gamma_0}{V_0}, \quad (7)$$

where γ_0 is the value at the standard condition.

Substituting Eqs. (5) and (6) into Eq. (2) results in an energy balance condition for the solution of V_1 and V_2 . With a given Hugoniot data point from the experiment (i.e., P_h and V_m are known), the left-hand side of Eq. (2) is determined by

$$E_m = \frac{1}{2} P_h (V_{01} - V_m), \quad (8)$$

where V_{01} is the specific volume of β -Si₃N₄ at zero pressure. The right-hand side, therefore, is a constraint on the ratio of V_1 and V_2 .

We have calculated the shock temperature T_{h1} (or T_{h2}) for each phase through

$$T_{h1} = T_s(V_1) + [E_1 - E_s(V_1)]/C_{v1}, \quad (9)$$

or

TABLE III. Physical parameters of β -Si₃N₄ and c -Si₃N₄ used and determined in this study, together with a comparison to the reports in literature.

| Phase | Density $\rho_0(\equiv 1/V_0)$ (g/cm ³) | Grüneisen ratio γ_0 | Specific heat C_v (J/g k) | Bulk modulus K_0 (GPa) | Pressure derivative K'_0 |
|---|---|----------------------------------|--------------------------------------|-----------------------------------|----------------------------------|
| β -Si ₃ N ₄ | 3.236 ^a | 1.1 ^b | 0.7 ^c | 232.7 ^d | 4.0 ^e |
| | 3.197 ^f | | | 270 ± 5 ^f | 4.0 ± 1.8 ^f |
| | 3.200 ^g | | | 259 ^g | |
| c -Si ₃ N ₄ | 4.012 ^h | 1.2 ^b | 0.7 ^c | 300 ± 10 ⁱ | 3.0 ± 0.1 ⁱ |
| | 3.930 ^j | | | 300 ^j | |
| | 3.873 ^{k,l} | | | 280 ^{k,l} | 3.48 ^k |

^aAveraged from SN-A samples.

^b $\gamma_0 = \alpha_v K_0 V_0 / C_v$, with $\alpha_v = 1.08 \times 10^{-5} \text{ K}^{-1}$ Ref. 2.

^cReference 2.

^dUltrasonic data, see Table I.

^eAssumed value, see the text and Fig. 4.

^fReference 7.

^gReference 22.

^hReference 9.

ⁱDetermined in this study, see the text.

^jReference 3.

^kReference 4.

^lReference 5.

$$T_{h2} = T_s(V_2) + [E_2 - E_s(V_2) - E_{tr}]/C_{v2}, \quad (10)$$

where C_v is the specific heat at constant volume, and $T_s(V)$ is the isentropic temperature determined by

$$T_s(V) = T_0 \exp \left[- \int_{V_0}^V \left(\frac{\gamma}{V} \right) dV \right], \quad (11)$$

with $T_0 = 293 \text{ K}$ being the initial temperature.

The parameters V_0 , γ_0 , and C_v for both β - and c -Si₃N₄ phases are listed in Table III. For β -Si₃N₄, there are compression reports from both static^{7,23} and shock wave⁸ studies. In Fig. 4, these data are compared with the present measurement at pressures below the phase transition point. A reasonable consistency between them is evident, but above HEL the static data indicate more stiffness than the shock compression data. A bulk modulus of $270 \pm 5 \text{ GPa}$, with the first pressure derivative of 4.0 ± 1.8 , was reported by Li *et al.*⁷ This value seems to be slightly high. A recent study by means of Brillouin scattering measurement has shown a bulk modulus of 259 GPa for a single crystal β -Si₃N₄.²⁴ In this study we used the bulk modulus of 232.7 GPa determined by the ultrasonic measurement (Table I). With an assumed pressure derivative of 4.0 , the isentrope of β -Si₃N₄ exhibits a good agreement with the shock compression data below the phase transition point (Fig. 4). Since there is no data available yet for the phase transition energy from β to c phase, the value of 821 J/g for the phase transition from α -quartz to stishovite²⁵ was adopted in the calculation. A similar structure transformation takes place but with all silicon atoms into octahedral coordinations linked with oxygen in the α -quartz to stishovite transition.

Calculation is performed with the set of equations from Eqs. (1)–(11), coupled with appropriate isentrope of c -Si₃N₄, to construct a theoretical Hugoniot curve for the mixed phase. Taking a reference Hugoniot data point from the experiment, V_1 and V_2 are first resolved from Eqs. (9) and (10) with a presumed shock temperature ($T_{h1} = T_{h2}$). These results (V_1 and V_2) are subsequently substituted into Eq. (1) to calculate λ , and into Eq. (2) to check the energy

balance condition. Adjustment of the shock temperature is repeated until the energy balance condition is satisfied within less than 1%. In Fig. 5, the dashed line is a computed Hugoniot curve which gives the best fit to the experimental Hugoniot data. The isentrope of c -Si₃N₄ deduced from this curve is shown in the same figure, for which a best fit with the Birch-Murnaghan EOS results in a bulk modulus and the first pressure derivative being 300 GPa and 3.0 , respectively, at zero-pressure and room temperature. The calculated mass fraction of c -Si₃N₄ in the mixed phases is depicted in Fig. 6. It increases monotonously with increasing shock pressure and shock temperature, and equals zero at the beginning of the mixed phase regime and one at the end.

The uncertainties of phase transition energy and specific heat may bring about possible errors in the above determination. These effects have been checked and they do not affect the calculated bulk modulus and the pressure derivative significantly. When E_{tr} is doubled from 821 to 1642 J/g ,²⁶ and C_v from 0.7 to 1.3 J/g k ,²⁷ the variations of K_0 and K'_0 are less than 3%. Therefore, we conclude that a bulk modulus of $300 \pm 10 \text{ GPa}$ with the first pressure derivative of 3.0 ± 0.1

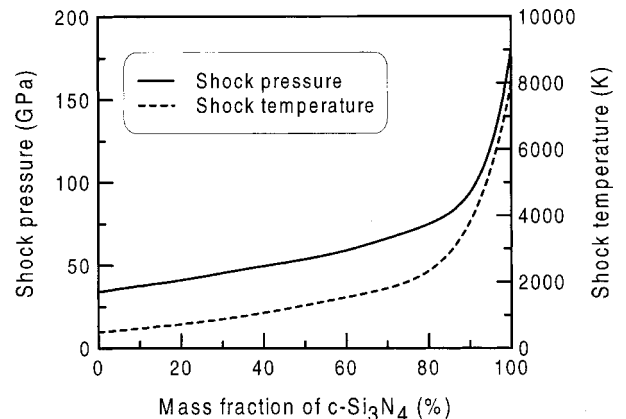


FIG. 6. Variation of mass fraction of c -Si₃N₄ in the mixed phase regime between 36.4 and 180 GPa, calculated with $K_0 = 300 \text{ GPa}$ and $K'_0 = 3.0$ for c -Si₃N₄.

can be inferred for c -Si₃N₄ from the present measurements. This result is in good agreement with the first-principles calculations³⁻⁵ (see Table III), which strongly indicates that c -Si₃N₄ is a low compressibility phase.

V. CONCLUSION

Hugoniot (pressure vs. density) data of β -Si₃N₄ has been determined up to the pressure 150 GPa. The phase transition from β - to c -Si₃N₄ has been observed at pressures above 36 GPa. This transition is very sluggish and appears to complete at about 180 GPa. Isentrope of c -Si₃N₄ has been deduced from the measurements, which gives the bulk modulus and its first pressure derivative to be 300 ± 10 GPa and 3.0

± 0.1 , respectively, at zero-pressure and room temperature. These values strongly support that c -Si₃N₄ is a low compressibility phase. Given the fact that the hardness of covalent materials increases with the bulk modulus,⁶ c -Si₃N₄ is expected to be a superhard material, comparable to stishovite.

ACKNOWLEDGMENTS

The authors gratefully acknowledge H. Otsuka for experimental assistance, and P. McMillan for discussion on the bulk modulus data on c -Si₃N₄. They thank Y. Horie for reviewing the draft.

*Author to whom correspondence should be addressed. Email address: sekine@nirim.go.jp

¹D. R. Messier and W. J. Croft, in *Preparation and Properties of Solid State Material*, edited by W. R. Wilcox (Marcel Dekker, Inc., New York and Basel, 1982), Vol. 7, p. 131.

²G. Ziegler, J. Heinrich, and G. Wötting, *J. Mater. Sci.* **22**, 3041 (1987).

³A. Zerr, G. Miehe, G. Serghiou, M. Schwarz, E. Kroke, R. Riedel, H. Fueß, P. Kroll, and R. Boehler, *Nature (London)* **400**, 340 (1999).

⁴S. D. Mo, L. Ouyang, W. Y. Ching, I. Tanaka, Y. Koyama, and R. Riedel, *Phys. Rev. Lett.* **83**, 5046 (1999).

⁵W. Y. Ching, L. Ouyang, and J. D. Gale, *Phys. Rev. B* **61**, 8696 (2000).

⁶J. M. Leger, J. Haines, M. Schmidt, J. P. Petitet, A. S. Pereira, and J. A. H. da Jornada, *Nature (London)* **383**, 401 (1996).

⁷Y. M. Li, M. B. Kruger, J. H. Nguyen, W. A. Caldwell, and R. Jeanloz, *Solid State Commun.* **103**, 107 (1997).

⁸A. Yamakawa, T. Nishioka, M. Miyake, K. Wakamori, A. Nakamura, and T. Mashimo, *J. Ceram. Soc. Jpn.* **101**, 1322 (1993).

⁹T. Sekine, H. He, T. Kobayashi, M. Zhang, and F. Xu, *Appl. Phys. Lett.* **76**, 3706 (2000).

¹⁰JCPDS card 33-1160.

¹¹I. Suzuki, H. Oda, S. Isoda, T. Sato, and K. Sey, *J. Phys. Earth* **40**, 601 (1992).

¹²T. J. Ahrens, W. H. Gust, and E. B. Royce, *J. Appl. Phys.* **39**, 4610 (1968).

¹³T. Sekine, S. Tashiro, T. Kobayashi, and T. Matsumura, *Shock Compression of Condensed Matter-1995* (AIP, New York, 1996), p. 1201.

¹⁴S. P. Marsh, *LASL Shock Hugoniot Data* (University of California Press, Berkeley, 1980).

¹⁵M. A. Meyers, *Dynamic Behavior of Materials* (Wiley-Interscience, New York, 1994), p. 101.

¹⁶R. G. McQueen, S. P. March, J. W. Taylor, J. N. Fritz, and W. J. Carter, in *High Velocity Impact Phenomena*, Chap. VII, edited by R. Kinslow (Academic, New York, 1970), p. 312.

¹⁷T. Sekine and T. Kobayashi, *Phys. Rev. B* **55**, 8034 (1997).

¹⁸M. Uchino, T. Mashimo, M. Kodama, T. Kobayashi, E. Takasawa, T. Sekine, Y. Noguchi, H. Hikosaka, K. Fukuoka, Y. Syono, T. Kondo, and T. Yagi, *J. Phys. Chem. Solids* **60**, 827 (1999).

¹⁹Y. Syono, K. Kusaba, K. Fukuoka, Y. Fukai, and K. Watanabe, *Phys. Rev. B* **29**, 6520 (1984).

²⁰J. P. Watt and T. J. Ahrens, *J. Geophys. Res. [Oceans]* **89**, 7836 (1984).

²¹H. Tan and T. J. Ahrens, *J. Appl. Phys.* **67**, 217 (1990).

²²J. W. Sweigle, *J. Appl. Phys.* **68**, 1563 (1990).

²³L. Cartz and J. D. Jorgensen, *J. Appl. Phys.* **52**, 236 (1981).

²⁴R. Vogelgesang, M. Grimsditch, and J. S. Wallace, *Appl. Phys. Lett.* **76**, 982 (2000).

²⁵R. A. Robie, B. S. Hemingway, and J. R. Fisher, *Thermodynamic Properties of Minerals and Related Substances at 298.15 K and 1 Bar (105 Pascals) Pressure and at High Temperatures* (United States Government Printing Office, Washington, 1978).

²⁶Compared with α -quartz to stishovite phase transition, both static and shock compressions indicate that higher pressure and temperature are required to promote the β - to c -Si₃N₄ transformation, which suggests that higher phase transition energy is expected for this transition.

²⁷I. Barin, in collaboration with F. Sauert, E. S. Rhonhof, and W. S. Sheng, *Thermochemical Data of Pure Substances Part II* (VCH Verlagsgesellschaft mbH, Weinheim, Federal Republic of Germany, 1989), p. 1357.